2023

Analysis of Biologically Effective Dose for Retroactive Yttrium-90 Trans-arterial Radioembolization Treatment Optimization

MJ Lindsey

Analysis of Biologically Effective Dose for Retroactive Yttrium-90 Trans-arterial Radioembolization Treatment Optimization

A Thesis Presented

by

Marcus (MJ) Lindsey

To the Keck Science Department
of
Claremont McKenna, Scripps, and Pitzer Colleges

In Partial Fulfillment of The Degree of Bachelor of Science
Senior Thesis in Biophysics

December 12th, 2022

Abstract

Trans-arterial radioembolization (TARE) is a protracted modality of radiation therapy where radionuclides labeled with Yttrium-90 (^{90}Y) are inserted inside a patient's hepatic artery to treat hepatocellular carcinoma (HCC). While TARE has been shown to be a clinically effective and safe treatment, there is little understanding of the radiobiological relationship between absorbed dose and tissue response, and thus there is no dosimetric standard for treatment planning. The Biologically Effective Dose (BED) formalism, derived from the Linear-Quadratic model of radiobiology, is used to weigh the absorbed dose by the time pattern of delivery. BED is a virtual dose that can be thought of as a common 'language' with which various forms of radiation therapy can use to 'communicate'. BED allows conclusions to be drawn about the biological response of TARE by putting it in conversation with what is known about the biological response of other treatment modalities, namely external beam radiation therapy (EBRT). A Python program was developed to calculate BED from absorbed dose distributions of six HCC patients treated at Massachusetts General Hospital, and optimized treatment activity levels with respect to biological response were determined. Within the limits of the BED analysis, none of the patients had originally received the optimal dose, with some patients having been overdosed and some having been underdosed. The results show there is a disconnect between the current clinical treatment planning standard for TARE and the tissue's biological response. This study suggests the need for patient-specific TARE dosimetry which considers biological response, such as BED or another adaptive model.

Table of Contents

1. Introduction

The field of medical physics is focused, generally, on the application of physics principles and methods for human disease prevention, diagnosis, treatment, and palliative care. There are several branches of study within medical physics, including medical imaging, nuclear medicine, and diagnostic medicine. However, one of the most prominent, and focus of this paper, is radiation oncology.

Radiation oncology applies the therapeutic properties of ionizing radiation, in various forms, to treat cancer in the human body. The goal of radiation therapy (RT) is to kill cancer cells and slow the growth of tumors by targeting and damaging their genetic material. There are a few different modalities for RTs, split into two main categories: external beam radiation therapies (EBRT), involving the use of a medical linear accelerator (LINAC) to eject high-energy particles into the human body, and brachytherapies (BT), involving the insertion of sealed radioactive materials into the body to provide a more concentrated and targeted dose to the tumor.

1.1 Yttrium-90 Trans-arterial Radioembolization

Trans-arterial radioembolization (TARE) is a form of BT wherein resin or glass microspheres containing Yttrium-90 (^{90}Y) radioisotopes are lodged within a patient's hepatic arteries to target hepatocellular carcinoma (HCC). The ^{90}Y radionuclides emit beta particles that destabilize the DNA structure of neighboring cells. This form of treatment is generally used for tumor downgrading as a bridge to surgery or palliation of the disease to provide comfort to the patient (Kim et al., 2019).

Currently, TARE is used to treat primary HCC, internal cholangiocarcinomas (ICC), neuroendocrine tumors (NETs) in the liver, and hepatic metastases. The high radiosensitivity of the liver parenchyma makes other EBRT treatments potentially dangerous, and the liver's unique vasculature structure makes TARE especially effective (Kim et al., 2019). The liver receives 75-80% of its blood supply from the portal vein, and the rest is supplied by the hepatic artery (Bierman et al., 1951). Conveniently, malignant hepatic tumors primarily perfuse from the hepatic artery and almost never from the portal vein (Van de Wiele et al., 2021). In many cases, this allows the radionuclides to be placed exclusively within the hepatic artery, providing dose to the roughly 20-25% of the liver where the tumors are located and sparing the healthy parenchyma (Kim et al., 2019).

As with any radiation therapy, TARE has a risk of radiation-induced toxicities. Riaz et al. (2014) provide a comprehensive explanation of these potential post-procedure challenges. While TARE has been shown to generally be safe, around 20 to 70% of patients will experience at least one complication. The most common complication is the post-radioembolization syndrome and is characterized by mild symptoms like fatigue, nausea, and abdominal pain. More severe complications are much less common, with an incidence rate of around 0 to 4%. Radiation-induced liver disease (RILD) can occur if the healthy parenchyma receives more than the tolerable dose. Another major concern is the development of radiation pneumonitis (RP), which is a risk when radionuclides escape into the lung's blood supply and provide unwanted dose to healthy lung tissue—a phenomenon called lung shunting. Extrahepatic radionuclide deposition also has a chance to occur within the gastrointestinal (GI) tract, often causing ulceration and bleeding.

Rigorous patient screening and pre-treatment procedures are done to avoid major complications like RILD, RP, and GI ulceration. The general clinical procedure, as outlined by Kim et al. (2019), begins with a screening process to filter out candidates with relevant contraindications for TARE. This includes patients with liver failure, patients who have previously had extensive EBRT for or around the liver, pregnant patients, and patients with a compromised portal vein.

Once a patient passes the initial screening, they undergo a series of pre-treatment scans and procedures to understand the patient's unique anatomy. The tumor and the liver parenchyma are first thoroughly outlined with a computerized tomography (CT) scan and magnetic resonance imaging (MRI). An angiography will then provide a patient-specific map of the hepatic vasculature and its hemodynamics. Knowing a patient's vasculature has several benefits: it guides where to insert the radionuclide delivery catheter, it provides information about the liver's blood flow, and it allows physicians to locate variance from the standard liver vasculature that could result in unexpected extrahepatic deposition or unwanted dose to the liver's healthy parenchyma (Kim et al., 2019).

The final pre-treatment step is single-photon emission computed tomography (SPECT) with CT (SPECT/CT) using the gamma-emitter Technetium-99m (^{99m}Tc) macroaggregated albumin (^{99m}Tc-MAA). ^{99m}Tc-MAA is similar in width as the ^{90}Y microspheres, with a diameter range of 15-150 μm, and its radioisotope component, ^{99m}Tc, has a short half-life of 6 hours (Gandhi et al., 2013). This makes ^{99m}Tc-MAA a good model for the ^{90}Y microsphere as it's easily imaged, it lodges similarly in the arteries, and it decays quickly enough to leave no clinical effect on the patient. ^{99m}Tc-MAA is injected into the hepatic arteries at the same location and angle that ^{90}Y radionuclides would be, and its

gamma rays produce an image that models how the therapeutic radionuclides would be distributed. A successful ^{99m}Tc-MAA image will confirm the results of the angiography and show any potential locations where extrahepatic deposition may occur.

Following these pre-treatment steps, the patient is cleared for treatment and the ^{90}Y microspheres are injected in an interventional procedure. The physician and physicist work together to prescribe and calculate the amount of radiation dose that the patient will receive, a field of study called dosimetry. Since ^{90}Y microspheres are calibrated in activity units, the current clinical standard for its dosimetry is a series of calculations, created by the Medical Internal Radiation Dose (MIRD) Committee and known as the MIRD schema, which derives a relationship between administered activity and absorbed dose (Kim et al., 2019). Dose to the liver is correlated to the injected activity of the radionuclides, the location of the radionuclides relative to the tumor, the mass of the tumor and the liver, and the expected amount of lung shunting.

There are a few known issues with TARE dosimetry, stemming mainly from the lack of uniform microsphere distribution in the liver. Since the microspheres travel through the hepatic arteries and lodge within the narrow arterioles, the microspheres will settle heterogeneously throughout the liver in clusters. However, the MIRD schema does not take the patient-specific vasculature and the spacing of the radionuclides into account, rather, it assumes a uniform dose to larger regions (Kim et al., 2019). Additionally, due to the delimitations of the liver and dose distribution, microspheres located around the tumor-tissue boundary, which may emit radiation between liver partitions, are unaccounted for in MIRD calculations. This phenomenon is called the 'crossfire effect' and is often cited to discredit the accuracy of the MIRD schema. As a result of the assumptions made to develop

the MIRD schema, its dose calculations are not always the most accurate. Nonetheless, due to its simplicity, MIRD is the clinical standard when treatment planning for TARE.

Imaging-based dosimetry is a patient-specific method used to calculate dose, and it is generally more accurate than the MIRD schema (Kim et al., 2019). This involves the use of SPECT/CT or Positron Emission Tomography (PET) with CT (PET/CT) images of dose distributions that are scaled by the administered activity to provide absorbed dose information. Since SPECT/CT images of the ^{99m}Tc-MAA distribution are acquired as part of the pre-treatment procedure, these images are sometimes used to calculate absorbed dose for the ^{90}Y treatment. While ^{99m}Tc-MAA and ^{90}Y radionuclides are not perfect matches in size, it is typically assumed that the variation between the two distributions is negligible (Kennedy et al., 2007). To convert the ^{99m}Tc-MAA activity maps to absorbed dose distributions, the MIRD schema is employed on the voxel level (Bertolet et al., 2021).

Imaging-based dosimetry is typically more accurate at measuring dose than the current clinical methods discussed above as it is patient-specific and does not rely on a generic model of dose distribution (Kim et al., 2019). By directly measuring the dose distribution with an image, the dose heterogeneity is accounted for, thus eliminating the need to worry about uniformity or crossfire effects. However, imaging-based dosimetry has tradeoffs, as it is limited by the resolution of the SPECT/CT image, which, with current technology, is not large enough to perfectly pinpoint where the microspheres are in the liver (Kim et al., 2019). Despite this, imaging-based dosimetry is still one of the most accurate ways to measure dose. As medical imaging technology advances, it is expected to only improve.

The most recent development in TARE dosimetry involves simulations of radionuclide activity using Monte Carlo (MC) methods. MC toolkits have been in development for several years, and some, like GEANT4 and TOPAS, are available to the public. A single simulation may perform millions of individual particle physics calculations to model how dose will accumulate over different geometries and mediums. MC simulations, when done over patient CT scans that provide information about tissue properties, have been shown to provide highly accurate dose distributions within clinical RT and are seen as the gold standard for measuring dose (Chetty et al., 2007). In addition, MC benefits over other forms of dosimetry as it works especially well in heterogenous tissue distributions, which are most accurate to the real tissues. The MC method has been shown to perform better than MIRD scheme-based dosimetry in TARE treatments as it provides more accurate dose distributions and extrahepatic deposition calculations (Bertolet et al., 2021).

Despite their clear advantages demonstrated in several small-scale studies, imaging-based dosimetry, whether found from MC simulations or voxel-wise MIRD calculation, have not generally been used in TARE treatment planning. While some clinics, to a limited extent, do utilize imaging-based dosimetry, it is far from the standard. However, in research, imaging-based dosimetry is popularly used to better understand radiation therapies and to determine directions for improving treatment effectiveness, patient safety, and patient experience.

1.2 The Linear-Quadratic Model and Biologically Effective Dose

Radiobiology is the branch of medical physics focusing on the action of ionizing radiation on biological tissues and their cellular and molecular components (Hall & Giacca, 2009). As it pertains to RT, this area of research is what motivates safer and more effective therapeutic techniques, treatment plans, and procedures. Radiobiological research in radiation oncology attempts to understand and model how the body and its numerous components react to various RT modalities. Biological effect models either employ biological theories to calculate radiobiological effects or are simply phenomenological and model what is seen empirically (Jones & Dale, 2018). Both methodologies have provided promising results and are often used in conjunction in contemporary radiobiological research.

There are five primary biological factors that must be taken into account when treatment planning, referred to as the five Rs of radiobiology: Radiosensitivity, which considers how different types of cells respond differently to radiation; Repair, which considers how DNA repairs the damage done by radiation; Repopulation, which considers how cells repopulate themselves in a tissue after others are killed by radiation; Redistribution, which considers how the distribution of cells at the most radiosensitive part of the cell cycle changes over time; and Reoxygenation, which considers how hypoxic cells become more sensitive to radiation once they reoxygenate (Herskind et al., 2017; Suntharalingam et al., 2005). The standard measurement of absorbed dose simply registers how much activity was absorbed in a tissue but does not consider these other biological factors that can drastically alter how the body responds.

The first factor, radiosensitivity, is important in treatment planning as it outlines how much dose a given tissue can receive within a safe limit. For example, the GI tract, composed of high radiosensitive cells, will have a greater response than muscle tissue, composed of low radiosensitive cells, if given the same dose. The last four of these factors describe how a tissue's radiosensitivity can change over time. In many RTs, it is standard to take advantage of this by fractionating the treatment into several smaller doses and delivering it over the course of several weeks to maximize the therapeutic potential of the treatment and minimize damage to healthy tissue. For example, a patient who receives 9 fractions of 5 Gy each over the course of two months will have a better outcome than a patient who receives the entire 45 Gy dose in one session despite both receiving the same total absorbed dose.

To understand this quantitatively, physicists have developed the Linear-Quadratic (LQ) model. The LQ model is the standard for modelling the effect of radiation dose on cell survival and tissue response (Jones & Dale, 2018). In short, it shows how the number of cell death events, E, has a linear-quadratic relationship with applied dose, D, and the radiosensitivity parameters of the tissue, α and β:

$$E = \alpha D + \beta D^2$$

The radiosensitivity parameters, α and β, reflect the inherent radiosensitivity of the tissue, with higher α and β values denoting higher sensitivity. They are found through in vitro studies of artificial tumor cell lines (Leeuwen et al., 2018). These cell line cultures, taken from samples of various tissue structures, are subjected to radiation doses and their cell death events are manually counted, allowing an LQ curve to be fit to the data.

While the LQ model is widely accepted, because of its empirical origins, its parameters do not reflect the underlying biological mechanisms which govern this response (Sgouros et al., 2021). Regardless, it still forms the foundation of most radiation biological effect models. Another useful value, the probability of a cell's survival, or the surviving fraction (SF), assuming the cell death events are Poisson distributed from cell to cell, is given by:

$$SF = e^{-(\#events)} = e^{-(\alpha D + \beta D^2)}$$

From this model of SF, shown in Figure 1, it is clear how fractionation of a treatment affects cell survival. The fractionated treatment is more sparing on the cells than the unfractionated treatment while still providing the same total absorbed dose to the tumor. It is important to note that this model assumes that there is enough time between fractions to allow full sublethal damage repair (Jones & Dale, 2018).

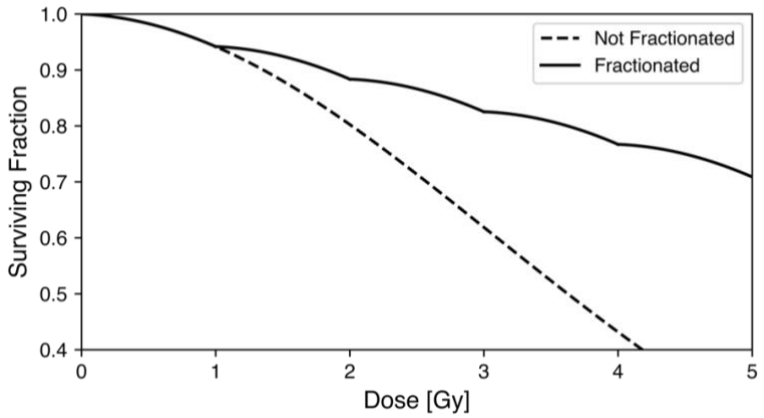

Figure 1 An exaggerated model of different surviving fraction curves which demonstrate how fractionation increases cell sparing effects

A more useful formulation of the SF model, including the effect of the irradiation time pattern, is Biologically Effective Dose (BED). BED intends to produce a virtual dose

weighting the applied dose by the time pattern of delivery (Fowler, 2010). For fractionated treatments, the specific radiosensitivity of the target tissue is considered by the α and β radiosensitivity parameters, and the other four time-dependent biological factors are considered by conservatively assuming an infinitely small dose rate, or dose per fraction. Since cell radiosensitivity fluctuates with time, assuming an infinitely small dose rate theoretically maximizes radiosensitivity by always having ionizing events occur when the cell is most vulnerable (Hall & Brenner, 1991).

BED has several clinical applications in fractionated treatment plans (Fowler, 2010). First, BED allows treatment plans with varying schedules to be easily compared since it converts all fractionation schedules to the same infinitely small dose rate. Second, in cases where a few fractions of a treatment were given erroneously, the schedule can easily be adjusted mid-treatment to provide the same BED. Finally, BED can be used post-clinically to analyze the treatment outcome.

BED is defined as the negative log of SF divided by α:

$$BED \equiv \frac{-\ln(SF)}{\alpha} = \frac{\alpha D + \beta D^2}{\alpha} = D\left(1 + \frac{D}{\frac{\alpha}{\beta}}\right)$$

For fractionated treatments of n fractions with a uniform dose per fraction, d, the total BED is the sum of the fractional BEDs:

$$BED_{tot} = \sum_n BED_n = nd\left(1 + \frac{d}{\frac{\alpha}{\beta}}\right) = D\left(1 + \frac{d}{\frac{\alpha}{\beta}}\right)$$

When discussing TARE treatments, however, dose is protracted over several days and is not fractionated. Recalling the assumption made in the SF model that, between fractions, the cells are given enough time to completely heal, TARE treatments cannot be appropriately modeled with this BED formula. To derive an equation for TARE BED, a time factor, $\Gamma(t)$, below, that considers the biological effect of partial DNA repair must be added to the LQ model (Brenner, 2008; Lea & Catcheside, 1942; Sgouros et al., 2021).

$$\Gamma(\tau) = \frac{2}{D^2}\int_0^{\tau} \dot{D}(t) \int_0^{t} e^{-\mu(t-t')}\, \dot{D}(t')dt'dt$$

The time factor is derived from the kinetic equations which govern the repair of double-strand breaks (DSB) in DNA (Brenner, 2008). DSBs are assumed to happen in two parts: the first of the breaks occurs at time t', and the second of the breaks occurs later and can interact with other first-breaks. The inner integral describes the first part of the DSBs and is composed of the dose rate in terms of the time of the first DSB event, $\dot{D}(t)$, and an exponential term that accounts for the reduction of DSBs as they are repaired. The exponential term includes the first-order rate constant for DSB DNA repair, μ. The outer integral describes the second part of the DSBs and comprises the dose rate and the inner integral. The $\frac{2}{D^2}$ term normalizes the time factor.

The time factor is applied to the quadratic term of the LQ model since DSBs and their repair are proportional to the square of the dose (Brenner, 2008). The time-dependent LQ model is thus:

$$E = \alpha D + \Gamma(\tau)\beta D^2$$

And the BED formula becomes:

$$BED = D\left(1 + \Gamma(\tau)\frac{D}{\frac{\alpha}{\beta}}\right)$$

In the case of TARE, the time factor can be reduced extensively. First, it is assumed that the gradually decreasing dose rate, $\dot{D}(t)$, is proportional to the exponential rate of decay of the radionuclides. Thus, dose rate, in terms of the decay constant, λ, and the initial dose rate, $\dot{D}_0$, is represented as:

$$\dot{D}(t) \;=\; \dot{D}_0\, e^{-\lambda t}$$

Second, since TARE is protracted until the radionuclides completely decay, the time factor can be evaluated at the limit $\tau \;\to \infty$. The time factor then reduces to:

$$\Gamma(\infty) = \frac{\lambda}{\lambda + \mu}$$

For convenience, we can rewrite the time factor in terms of the radionuclide's half-life, $T_{half-life}$, and the DNA's repair half-time, T_{repair}, using their relationships to μ and λ respectively:

$$T_{half-life} \;=\; \frac{ln(2)}{\mu}$$

$$T_{repair} \;=\; \frac{ln(2)}{\lambda}$$

Thus, our final formulation of the time factor is:

$$\Gamma(\infty) = \frac{T_{repair}}{T_{repair} + T_{half-life}}$$

And our equation for TARE BED is:

$$BED = D\left(1 + \frac{D}{\frac{\alpha}{\beta}} \cdot \frac{T_{repair}}{T_{repair} + T_{half-life}}\right)$$

Contrasting the multiple clinical applications of BED for fractionated treatments, TARE BED is rarely, if ever, used clinically as there is a severe lack of literature detailing the clinical benefits of BED for TARE treatment planning. However, TARE BED does have applications in research. By comparing the BED of better-researched radiation treatment modalities, like EBRT, to the BED of TARE, we can make judgements about the biological effect of protracted treatments, which is integral to the development of safer and more effective TARE treatments.

Clearly shown in the equation for BED is its dependence on the ratio of the radiosensitivity parameters, α/β. The tissue's α/β ratio describes its responsiveness to fractionation (Leeuwen et al., 2018). A tissue with a low α/β ratio (β is high) benefits more from fractionation since its SF curve has more quadratic character and is thus steeper. Conversely, a tissue with a high α/β ratio (α is high) benefits less from fractionation since its SF curve has more linear character and is thus shallower. This phenomenon is demonstrated in Figure 2.

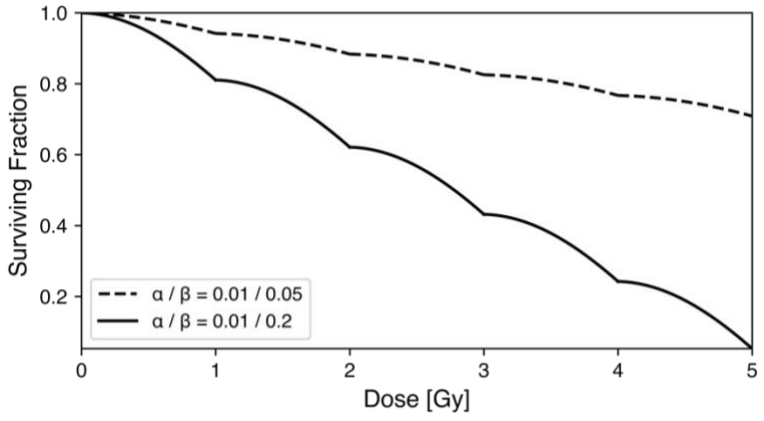

Figure 2 A model of surviving fraction for two different treatments. Each treatment has five fractions, but the tissues have different α/β ratios. The large α/β ratio creates a shallow curve, while the small α/β ratio creates a steep curve.

There are a few problems to note with the radiosensitivity parameters and the available literature surrounding them. First, the empirical nature of their derivation and their lack of a relationship to fundamental biophysical concepts introduces a level of uncertainty that should be acknowledged when applying them in LQ models (Sgouros et al., 2021). Second, there are few studies available that have published their findings for these parameters, making it difficult to obtain a good average value for most tumor types and tissues (Leeuwen et al., 2018). Finally, of the literature that is available of these values, there is a high degree of study heterogeneity (Leeuwen et al., 2018). This means that there is more variation between different studies of reported radiosensitivity parameters than is statistically expected, essentially preventing the establishment of well-defined α and β values for individual tissue and tumor types. Since BED is only as accurate as the α and β values chosen, it should generally only be taken as a guideline measurement.

While α and β values and the α/β ratio are not conclusive measurements, there are a few accepted trends for α/β ratios. As explained previously, the ratio of the radiosensitivity parameters describes the sensitivity to fractionation. The tissues most protected by fractionation, known as late-responding tissues, are typically normal tissues, whereas the tissues least protected, known as early-responding tissues, are typically tumors (Williams et al., 1985). While this is not true for all types of tissues and tumors, most of them follow this trend (Hegemann et al., 2014; Leeuwen et al., 2018). Therefore, tumors will generally have a high α/β ratio ($\alpha/\beta \sim 10$) and normal tissues will have a low α/β ratio ($\alpha/\beta \sim 3$).

1.3 Research Topic

The goal of this paper is to quantitatively demonstrate how TARE BED can be used to create safer and more effective treatments. To do this, I analyzed the BED of six different HCC patients treated with ^{90}Y TARE at Massachusetts General Hospital (MGH) in Boston, MA. By analyzing the BED of past TARE treatments, it is possible to conclude ways the treatment might be better optimized to target the tumor and preserve the surrounding healthy tissue more effectively. This project was done under the guidance of Dr. Alejandro Bertolet, PhD, who leads a lab at MGH that studies radiation oncology physics to develop better outcomes, higher quality of life, and more effective treatments for patients.

I first developed a program to calculate BED distributions from voxelized absorbed dose distributions. The absorbed dose distributions were previously calculated by Bertolet using SPECT/CT ^{99m}Tc-MAA activity-map images and TOPAS MC accumulated dose simulations (Bertolet et al., 2021). Once BED is calculated, BED in the normal liver was compared to the accepted maximum dose as set by the Quantitative Analysis of Normal Tissue Effects in the Clinic (QUANTEC) studies. While the QUANTEC standards are written for EBRT treatments given in 2 Gy fractions, by converting the standard to its equivalent in BED we can effectively draw conclusions about TARE dose tolerances. I used the relationship between dose and injected activity to retroactively determine an activity level that would provide this maximum tolerance dose to the liver, thus maximizing the dose to the tumor while still protecting the liver parenchyma.

Since the original treatment was not planned with BED in mind, a measurable difference in the actual applied activity and the optimal theoretical activity was expected.

This paper is meant to provide insight into the clinical potential of BED for TARE treatments.

2. Experimental Design and Python Application

This study aims to calculate BED for TARE to make claims about the effectiveness and safety of the treatment modality. To accomplish this, I developed a Python application that calculates TARE BED distributions from absorbed dose distributions. This application was used to calculate the BED for six HCC patients that were previously treated at MGH. The BED distributions and subsequent plots created to analyze them were calculated using the radiosensitivity parameter ratios, α/β, T_{repair}, and $T_{half-life}$, shown in Table 1. To determine the appropriate radiosensitivity parameters, a brief review of current literature was done, and the averages for the parameter values determined in previous studies were calculated.

Table 1 Mean α/β ratios and T_{repair} used in BED calculation [Kehwar, 2005; Kirkpatrick et al., 2008; Leeuwen et al., 2018, Michel et al., 2017; Orton, 2001; Son et al., 2013]

	Site	Mean α/β	T_{repair}
Normal	generic	3	2.5
	liver	2.75	
Tumor	generic	10	1.5
	liver	10	

The Python application was written as an addition to MGH's open-source medical imaging processing software. Both the original source-code and the BED application can be found at https://github.com/mghro/MIRDCalculation. The software handles medical images stored using the Digital Imaging and Communications in Medicine (DICOM) protocol: the clinical standard for storing, viewing, and transmitting medical images. DICOM files combine 2D and 3D images, image metadata, and patient-specific information into a single package. There are two main types of DICOM files: RTSTRUCT, which stores the shape and location, often called contours, of regions of interest (ROI), and RTDOSE, which stores dose distributions.

MGH's original software provides the tools for reading and writing various DICOM files. My application utilizes these to produce the BED distributions as RTDOSE outputs. It has three inputs: a CT image, an RTSTRUCT, and an RTDOSE. The CT image input defines the voxel grid layout onto which the other two files are overlayed. The RTSTRUCT input contains a set of bitmaps which define the voxelized shape of each ROI and their location on

the CT. The RTDOSE input contains the voxelized absorbed dose distribution. Together, these three files provide all the information needed to calculate the BED distribution.

Below is the script which calls the three main functions created to calculate BED: *BEDCalculator.__init__( )*, *BEDCalculator( )*, and *WriteRTDoseBED( )*. The file path to the input DICOM files is provided here, along with the desired dose unit for the output BED RTDOSE.

```
# 1. Path to DICOM files (str)
basepath = '/Users/mjlindsey/Documents/LiverPatients/Patient1/POSTTX/'

# 2. RTDOSE filename (str)
dosefile = 'MIRDDose.dcm'

# 3. Units for BED RTDOSE file (str) (Choose from "Gy/GBq", "Gy/mCi", or
"Gy")
unit = 'Gy/GBq'

### Main Script ###
calc = BEDCalculator(basepath, dosefile, unit)
calc.BEDCalculator()
calc.WriteRTDoseBED()
```

The first function, *BEDCalculator.__init__( ),* initializes the BEDCalculator class. First, the CT metadata is read to determine the voxel dimensions. Then, the RTSTRUCT is converted to a dictionary of 3D arrays for each ROI, and the RTDOSE is converted to a single 3D array. If necessary, these are scaled to match the dimensions of the CT. This is the most convenient way to access the information for BED calculation as it allows each voxel to be indexed for its unique tissue identity and dose value. Additionally, the application provides a way for the unit of the input RTDOSE to be converted if it differs from the chosen unit for the BED RTDOSE.

```
class BEDCalculator(dcmpat.PatientCT):
```

```
    def __init__(self, basepath, dosefile, unit = "Gy/GBq", maxVoxel =
None):
        self.unit = unit
        if maxVoxel != None:
            self.maxvoxel = maxVoxel
        ctpath = basepath + '/CT/'
        dosepath = basepath + dosefile
        dosefile_full = os.path.basename(dosefile)
        dosefile_split = dosefile_full.split('.')[0]
        self.basepath = basepath
        self.dosefilename = dosefile_split
        self.patientObject = dcmpat.DicomPatient(basepath)
        self.patientObject.dcmFileChosen = pydicom.dcmread(dosepath)
        self.ctObject = dcmpat.PatientCT(ctpath)
        self.ctObject.LoadRTDose(dosepath)
        try:
            structfile = os.listdir(basepath + '/RTSTRUCT/')
            structpath = basepath + '/RTSTRUCT/' + structfile[0]
            self.ctObject.LoadStructures(structpath)
        except Exception as e:
            structfile = os.listdir(basepath + '/RTSTRUCT_LUNGSANDLIVER/')
            structpath = basepath + '/RTSTRUCT_LUNGSANDLIVER/' +
structfile[0]
            self.ctObject.LoadStructures(structpath)
            print('ERROR: Could not load complete RTSTRUCT. CODE:', e)
            print('RTSTRUCT_LUNGSANDLIVER loaded instead.')
        self.ROIs = list(self.ctObject.structures3D.keys())
        print("ROI's identified:", self.ROIs)
        self.TUMORS = []
        for STRUCT in self.ROIs:
            if 'Tumor' in STRUCT:
                self.TUMORS.append(STRUCT)
        print("Tumor STRUCTS identified:", self.TUMORS)
        self.BEDimg3D = np.zeros(self.ctObject.img3D.shape)
        self.ConvertDoseUnits()
```

Once the CT, RTSTRUCT, and RTDOSE have been loaded, the BED distribution is calculated. First, the program iterates voxel-wise through the RTDOSE array. At each index, the program confirms from the RTSTRUCT dictionary which ROI the voxel is within. This allows the program to define the appropriate α/β ratio and T_{repair} for the BED calculation at that voxel. The BED value is stored into a separate 3D array, and the program continues to the next voxel.

```
def BEDCalculator(self):
        for i in
range(self.ctObject.quantitiesOfInterest[0].array.shape[0]):
            if (i % 20) == 0:
                prog =
i/self.ctObject.quantitiesOfInterest[0].array.shape[0]*100
                print("Calculating BED... (" + str(round(prog,1))+"%)")
            else:
                pass
            for j in
range(self.ctObject.quantitiesOfInterest[0].array.shape[1]):
                for k in
range(self.ctObject.quantitiesOfInterest[0].array.shape[2]):
                    if self.ctObject.structures3D['Liver'][i,j,k] == True
:
                        for t in self.TUMORS:
                            if self.ctObject.structures3D[t][i,j,k] ==
True:
                                Trep = Trep_Tumor
                                AlphaBeta = AlphaBeta_TLiver
                                break
                            else:
                                Trep = Trep_Normal
                                AlphaBeta = AlphaBeta_NLiver
                    elif self.ctObject.structures3D['Lung_L'][i,j,k] ==
True or self.ctObject.structures3D['Lung_R'][i,j,k] == True :
                        Trep = Trep_Normal
                        AlphaBeta = AlphaBeta_NLung
                    else :
                        Trep = Trep_Normal
                        AlphaBeta = AlphaBeta_Standard
                    self.BEDimg3D[i,j,k] =
self.ctObject.quantitiesOfInterest[0].array[i,j,k] * (1 + ((
self.ctObject.quantitiesOfInterest[0].array[i,j,k] * Trep) / (AlphaBeta *
(Trep + RadionuclideHalfLife))))
        print('BED Calculated.')
```

After the BED has been calculated for each voxel, the resultant BED array is written as a new RTDOSE file.

```
def WriteRTDoseBED(self, seriesdescription = None):
        if seriesdescription == None:
            seriesdescription = 'BED_' + self.dosefilename
        name = 'BED_' + self.dosefilename + '.dcm'
        self.ctObject.WriteRTDose(self.BEDimg3D, self.basepath + name,
self.unit, seriesdescription)
```

This application was used to calculate the BED distribution for each of the six patients. Once these were obtained, comparative dose-volume histograms (DVH), which provide information about dose concentration within ROIs, were calculated using 3D Slicer medical imaging software. Finally, activity-dose plots showing how dose to the BED of the normal liver and liver tumor scale with activity were created for each patient. These were created by measuring the mean BED at various activity levels for each ROI. The optimal activity was chosen to be the activity which provided a mean BED to the normal tissue of 70 Gy[BED], which is the level as reported by QUANTEC that will induce RILD 50% of the time.

3. Results

Figure 3 shows the absorbed dose and BED distributions for each patient. As expected, the normal tissues show a larger increase in dose value between absorbed dose and BED than the tumors.

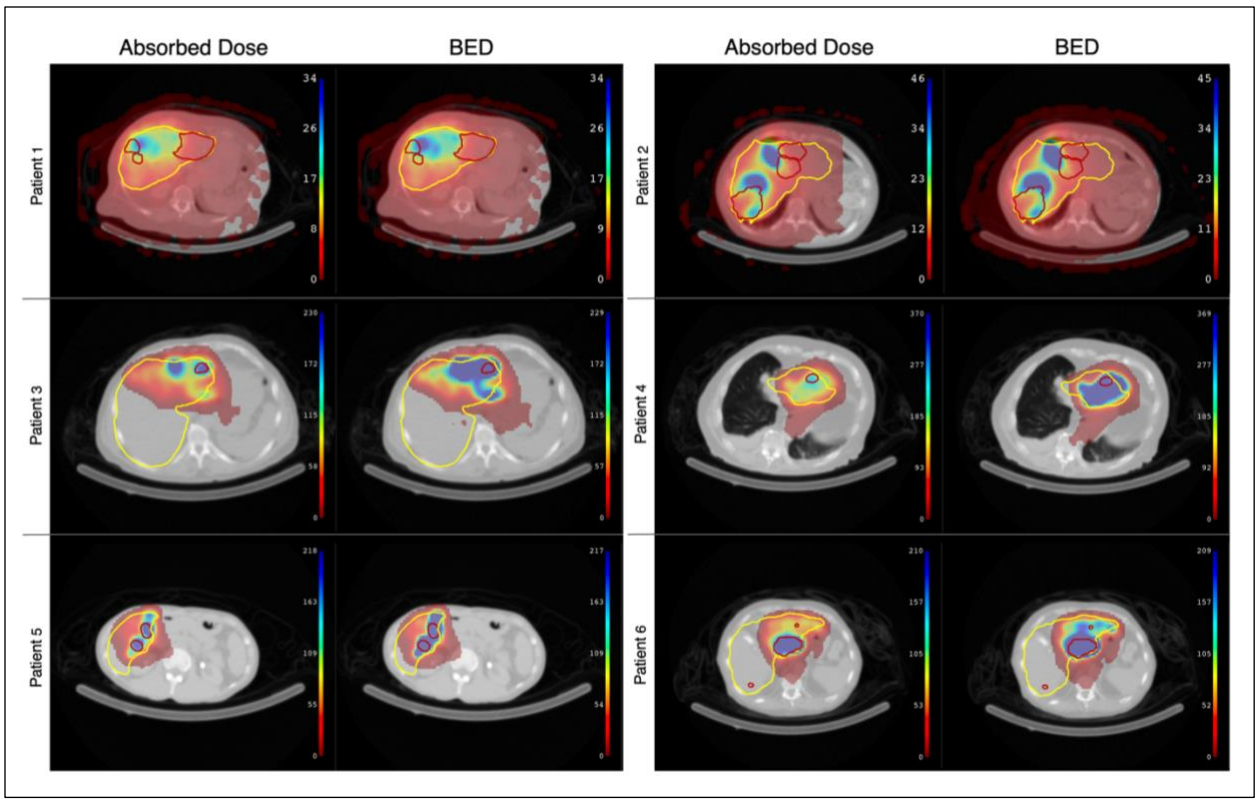

Figure 3 Distributions of absorbed dose (left) and biologically effective dose (right) in an axial plane for each patient. The liver is represented by yellow contours, and tumors are represented by red contours.

Figures 4 shows the DVHs comparing absorbed dose and BED for each patient. The non-linear transformation from absorbed dose to BED is demonstrated here, as larger absorbed dose values are scaled up more than lower absorbed dose values. This is seen further in Figure 5, which shows the absorbed dose and BED activity-dose curves for each patient. The absorbed dose scales linearly with increasing activity whereas the BED expectedly follows a linear-quadratic pattern as activity increases. Finally, Figure 6 shows the difference between the optimal activity and the actual activity used overlayed onto the BED activity-dose curves.

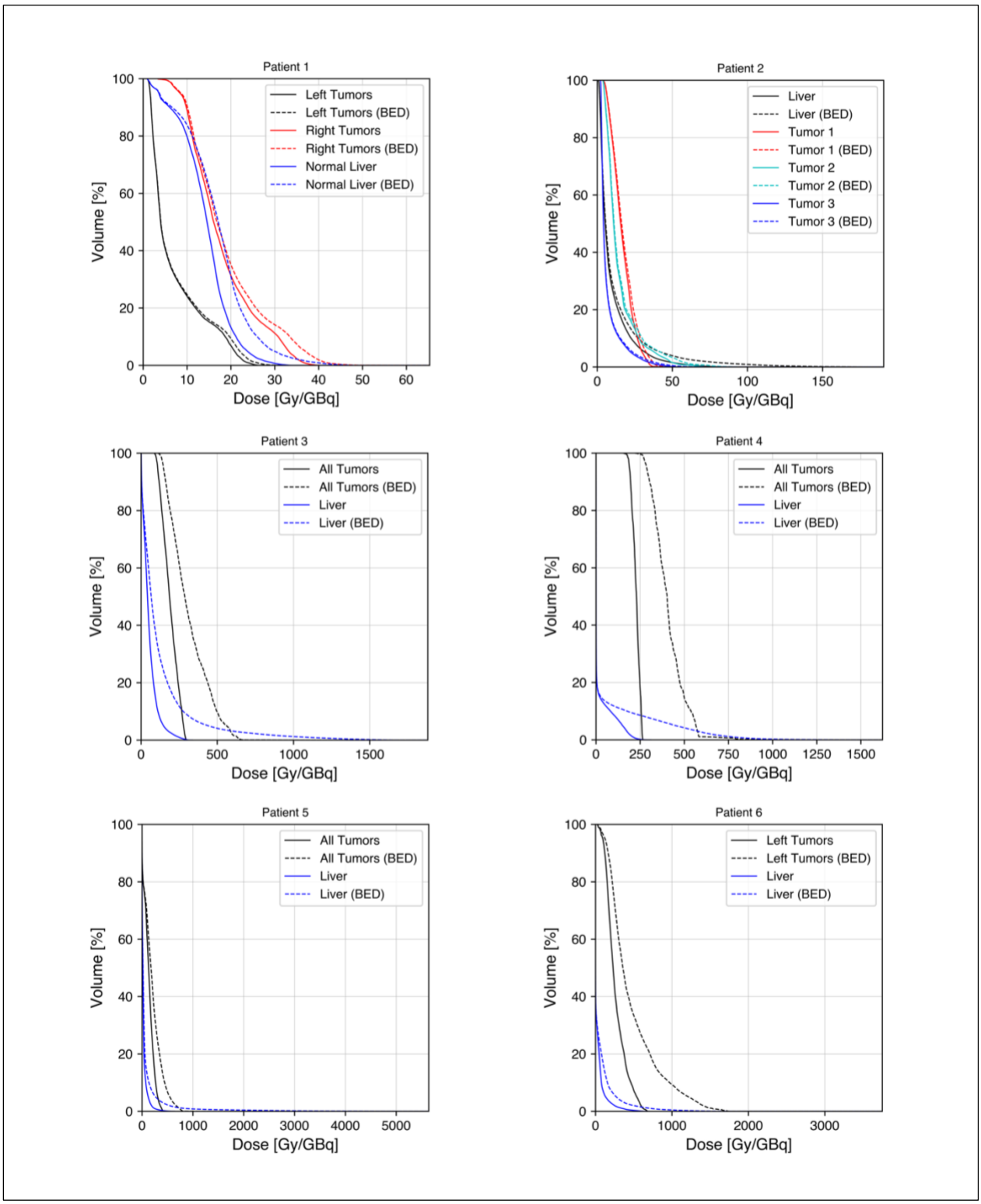

Figure 4 Dose-volume histograms for absorbed dose and biologically effective dose per activity.

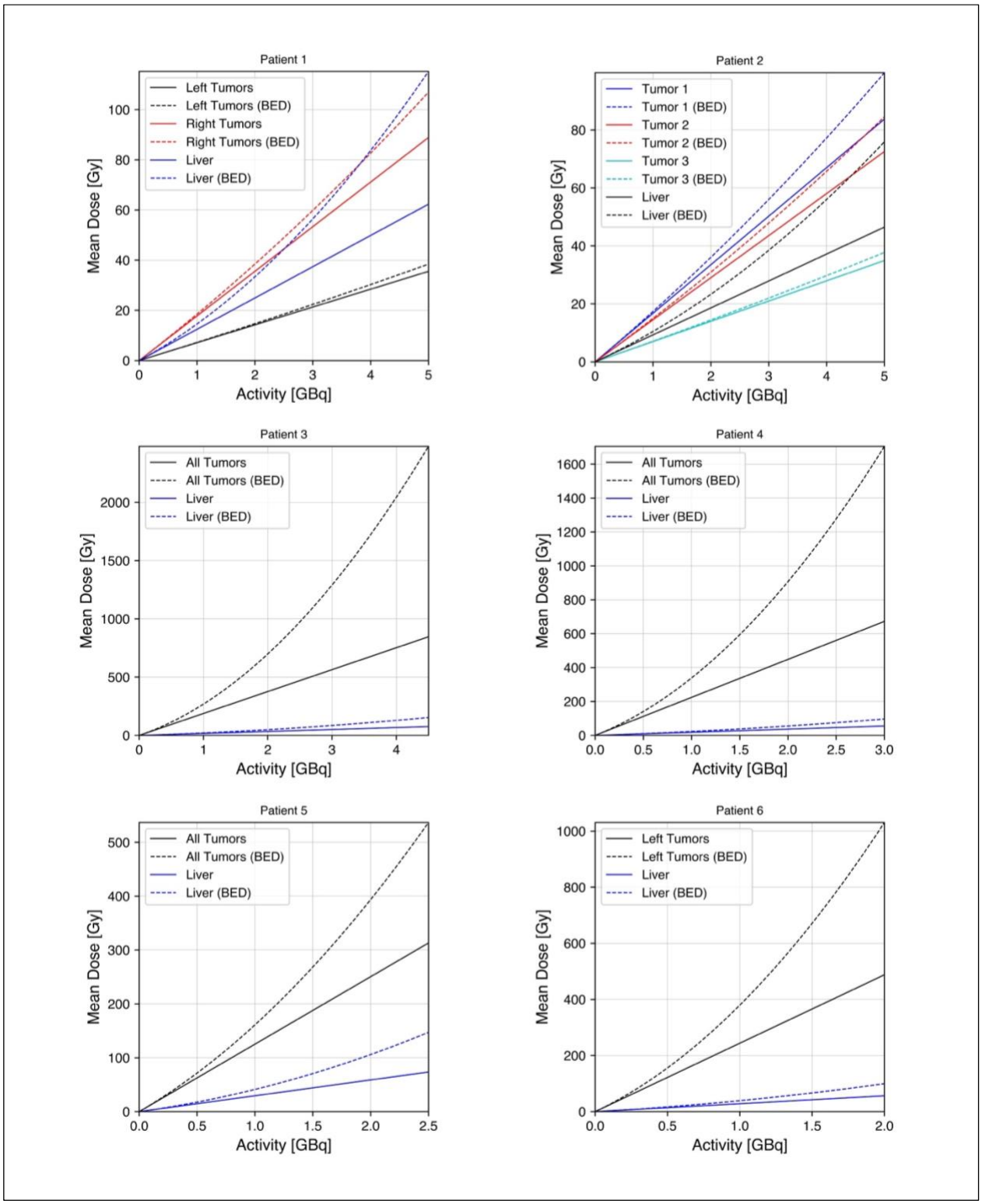

Figure 5 Activity-dose curves for absorbed dose and biologically effective dose.

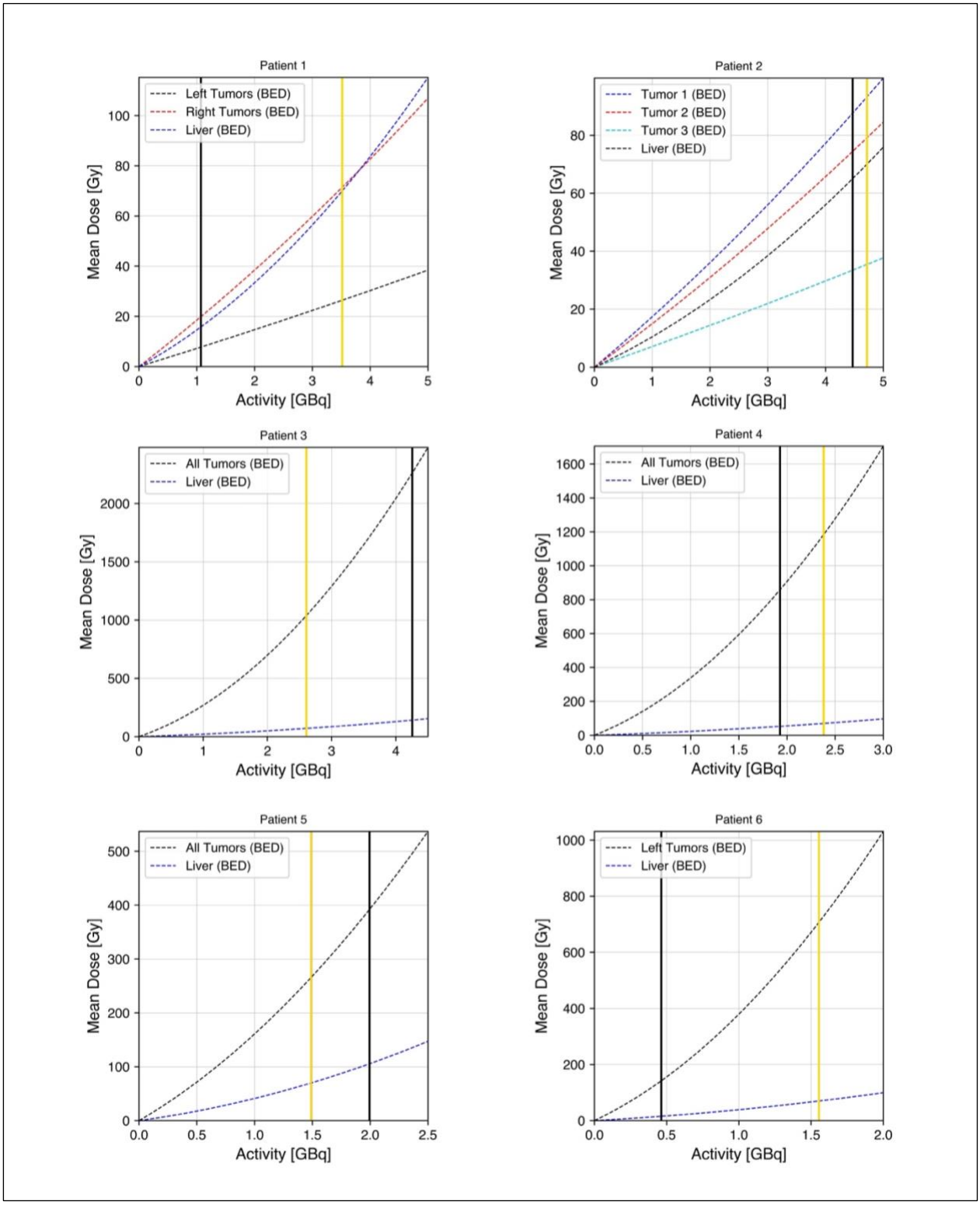

Figure 6 Activity-dose curves for biologically effective dose. The vertical bars represent the activity level that was applied, in black, and the optimal activity according to the BED treatment analysis, in gold.

4. Discussion

4.1 Analysis of Results

The results of this study highlight the importance of considering biological effect in the treatment planning of TARE. As shown in Figures 3, 4, and 5, different tissue types and volumes scale differently when converting from absorbed dose to BED, with normal tissue showing the largest increase. This is as expected and confirms that the calculations for BED were correct. As shown in Figure 6, mixed results were found when optimizing the activity for each patient. Assuming that the LQ and BED models are correct and that the QUANTEC dose threshold values are applicable to all patients, we can conclude that none of the patients had originally received the optimal dose.

While there is no significant trend in either one direction, the wide differences between administered activity and the optimal activity are concerning. In patients 1, 3, and 6, the difference between the administered activity and the optimal activity is greater than 1 GBq, which is a substantial amount. Without data about specific patient outcomes or metrics like tumor reduction and prevalence of complications, it is difficult to claim the severity of these gaps between the activities. However, since the optimal activity was set to the dose which would on average induce RILD 50% of the time, it is appropriate to conclude that the patients who were overdosed had a much higher chance of developing RILD or another related complication. For the patients who were underdosed, we can conclude that the tumors were likely not treated to the highest extent possible, and the patients could have handled more rigorous treatments.

This study suggests the need for patient-specific treatment planning which considers biological effect. Had each patient initially received a personalized dosimetric

work-up like those performed in this study to develop a treatment plan based on the patient's unique biological composure, these large gaps between the administered activity and the optimal activity would likely be reduced or eliminated completely.

4.2 Limitations

The conclusions drawn from this study are restricted by the limitations of the LQ and BED models. As discussed previously, the LQ model was created through empirical analysis of radiation-induced cell deaths. While the model does closely predict the rate of cell deaths, the formulation and associated α and β radiosensitivity parameters have no underlying biophysical definition. Additionally, within the available literature, there is still significant variance in the α and β values derived through experimental approximation. As the BED model relies on the accuracy of these radiosensitivity parameters, any conclusions drawn from it must consider this uncertainty.

A second limitation of this study is its scale. While the study of six patients demonstrated several key trends of TARE BED, a larger study is necessary to make claims about the clinical necessity of considering BED when planning TARE treatments. Studying more patients would provide a better average outcome and strengthen the efficacy of the BED analysis. Additionally, without patient outcome data, the conclusions made from this study were only general claims. For example, we might expect patients who were underdosed to have had less tumor reduction and patients who were overdosed to have experienced more post-procedure complications. However, without this information there is no way to confirm or deny these expectations. To draw more definite conclusions about the efficacy of TARE BED treatment planning, a large, multi-year study that tracks key

patient outcome and quality of life information, including fraction of tumor reduction, fraction of parenchyma sparing, rate of tumor recurrence, and rate of post-treatment complications, is necessary.

4.3 Conclusions and Future Work

This study made clear the benefits of radiobiological considerations in treatment planning for TARE patients. Since the BED of a given TARE treatment can vary significantly from the absorbed dose, the evidence supports the clinical use of BED in TARE dosimetry as a method for better treatment optimization. Further, as shown by the variations in biological effect between each of the six patients, individualized biological effect analyses should be done for each patient to account for their unique biology.

To increase the use and efficacy of BED in TARE treatment planning, a more robust understanding of the radiobiology of the liver and other human tissues is necessary. A model of biological effect that is based in radiobiological principles could provide a level of accuracy that is not currently possible within the standard LQ model. However, there are a few problems with the derivation of this approach. As discussed previously, the five most important radiobiological factors that would need to be considered are radiosensitivity, repair, repopulation, redistribution, and reoxygenation. The LQ model provides a good approximation for the average of these effects, but to produce a more accurate result it would be necessary to consider each of these factors individually. Even within a single cell, this proves difficult to compute (Cruz, 2016). This approach becomes nearly impossible when considering how many single-cell computations would be needed to account for the entire treatment area of the patient.

Analytically, the LQ model provides the most practical method of deriving BED. However, there is a developing project to predict the biological effect of a RT at the cellular and DNA level using MC simulations. This method completely circumvents the need for complex microdosimetry by allowing the accumulated behavior of the simulation to precisely show what will happen within the cell. Toolkits like GEANT4-DNA and TOPAS-nBio, which are publicly available addons to the GEANT4 and TOPAS softwares, provide the capability to simulate the effects of individual radiation moments to many different cell and DNA types (Schuemann et al., 2018). In this way, these toolkits can quantitatively determine the number of DSBs, thus deriving the number of cell deaths and radiosensitivity of a set of cells. Further, these toolkits can simulate DNA repair kinetics, directly measuring the relationship between DNA damage and repair—a key component of BED. Future versions of these toolkits have the potential to simulate the other radiobiological factors as well.

In addition, the cellular simulation models avoid the resolution limitations of the CT scan for imaging-based models. While a standard CT voxel will have a minimum width of about 0.5 mm, the size of a geometry in TOPAS-nBio can be scaled as small as desired, down to the width of a single DNA strand (Scheumann et al., 2018). Moreover, TOPAS-nBio implements cellular geometries that are curved, which is a more accurate depiction of tissues and tumors than the jagged, voxelized edges of a CT.

While it would incur a large processing cost, in theory, large-scale models of tissues could be built with each individual cell rendered separately. With a human body modeled in this hyper-realistic way, it would be possible to simulate a RT from the bottom-up, quantitatively measuring the exact biological effect, in terms of DSBs or cell deaths, of each

radiative transfer. A toolkit of this precision would be invaluable to the study of radiobiology, and many radiobiologists see its development as one of the next main goals of the field.

Although progress has been made with the GEANT4-DNA and TOPAS-nBio projects in creating bottom-up radiobiology toolkits, there is still much more research that must be done and many regulatory barriers to tackle before this type of treatment modeling could be applied clinically. Even when based in the LQ and BED models, which are applied often in EBRTs, there still is no standard to account for biological effect in TARE treatment planning. Considering all the time, effort, and money that would need to be invested in clinical trials to alter the standard procedure for TARE, it would require a significant breakthrough in the radiobiology of the treatment that substantially betters outcomes or quality of life. Due to this, it is highly unlikely TARE BED will be implemented anytime soon. However, as more is discovered about the biological effect of TARE treatments, changes in its clinical procedure are inevitable.

5. References

Bertolet, A., Wehrenberg-Klee, E., Bobić, M., Grassberger, C., Perl, J., Paganetti, H., & Schuemann, J. (2021). Pre- and post-treatment imaging-based dosimetry in ^{90}Y-microsphere radioembolization using the TOPAS Monte Carlo toolkit. *Physics in Medicine &Amp; Biology*, *66*(24), 244002. https://doi.org/10.1088/1361-6560/ac43fd

Bierman, Howard R., Byron, Ralph L., Kelley, Keith H., Grady, Alice. (1951). Studies on the Blood Supply of Tumors in Man. III. Vascular Patterns of the Liver by Hepatic Arteriography. *JNCI: Journal of the National Cancer Institute*. https://doi.org/10.1093/jnci/12.1.107

Brenner, D. J. (2008). The Linear-Quadratic Model Is an Appropriate Methodology for Determining Isoeffective Doses at Large Doses Per Fraction. *Seminars in Radiation Oncology*, *18*(4), 234–239. https://doi.org/10.1016/j.semradonc.2008.04.004

Chetty, I. J., Curran, B., Cygler, J. E., DeMarco, J. J., Ezzell, G., Faddegon, B. A., Kawrakow, I., Keall, P. J., Liu, H., Ma, C. M. C., Rogers, D. W. O., Seuntjens, J., Sheikh-Bagheri, D., & Siebers, J. V. (2007). Report of the AAPM Task Group No. 105: Issues associated with clinical implementation of Monte Carlo-

based photon and electron external beam treatment planning. *Medical Physics*, *34*(12), 4818–4853. https://doi.org/10.1118/1.2795842

Cruz, Santa G. A. (2016). Microdosimetry: Principles and applications. *Reports of Practical Oncology &Amp; Radiotherapy*, *21*(2), 135–139. https://doi.org/10.1016/j.rpor.2014.10.006

Fowler, J. F. (2010). 21 years of Biologically Effective Dose. *The British Journal of Radiology*, *83*(991), 554–568. https://doi.org/10.1259/bjr/31372149

Gandhi, S., Babu, S., Subramanyam, P., & Sundaram, P. (2013). Tc-99m macro aggregated albumin scintigraphy - indications other than pulmonary embolism: A pictorial essay. *Indian Journal of Nuclear Medicine*, *28*(3), 152. https://doi.org/10.4103/0972-3919.119546

Hall, E. J., Brenner, D. J. (1991). The dose-rate effect revisited: Radiobiological considerations of importance in radiotherapy. *International Journal of Radiation Oncology*Biology*Physics*, *21*(6), 1403–1414. https://doi.org/10.1016/0360-3016(91)90314-t

Hall, E. J., Giaccia, A. J., PhD. (2006). *Radiobiology For The Radiologist* (6th ed.). Lippincott Williams & Wilkins.

Hegemann, N. S., Guckenberger, M., Belka, C., Ganswindt, U., Manapov, F., & Li, M. (2014). Hypofractionated radiotherapy for prostate cancer. *Radiation Oncology*, *9*(1). https://doi.org/10.1186/s13014-014-0275-6

Herskind, C., Ma, L., Liu, Q., Zhang, B., Schneider, F., Veldwijk, M. R., & Wenz, F. (2017). Biology of high single doses of IORT: RBE, 5 R's, and other biological aspects. *Radiation Oncology*, *12*(1). https://doi.org/10.1186/s13014-016-0750-3

Jones, B., Dale, R. (2018). The evolution of practical radiobiological modelling. *The British Journal of Radiology*, 20180097. https://doi.org/10.1259/bjr.20180097

Kehwar, T. (2005). Analytical approach to estimate normal tissue complication probability using best fit of normal tissue tolerance doses into the NTCP equation of the linear quadratic model. *Journal of Cancer Research and Therapeutics*, *1*(3), 168. https://doi.org/10.4103/0973-1482.19597

Kennedy, A., Nag, S., Salem, R., Murthy, R., McEwan, A. J., Nutting, C., Benson, A., Espat, J., Bilbao, J. I., Sharma, R. A., Thomas, J. P., & Coldwell, D. (2007). Recommendations for Radioembolization of Hepatic Malignancies Using Yttrium-90 Microsphere Brachytherapy: A Consensus Panel Report from the Radioembolization Brachytherapy Oncology Consortium. *International Journal of Radiation Oncology*Biology*Physics*, *68*(1), 13–23. https://doi.org/10.1016/j.ijrobp.2006.11.060

Kim, S. P., Cohalan, C., Kopek, N., & Enger, S. A. (2019). A guide to 90Y radioembolization and its dosimetry. *Physica Medica*, *68*, 132–145. https://doi.org/10.1016/j.ejmp.2019.09.236

Kirkpatrick, J. P., Meyer, J. J., & Marks, L. B. (2008). The Linear-Quadratic Model Is Inappropriate to Model High Dose per Fraction Effects in Radiosurgery. *Seminars in Radiation Oncology*, *18*(4), 240–243. https://doi.org/10.1016/j.semradonc.2008.04.005

Lea, D. E., & Catcheside, D. G. (1942). The mechanism of the induction by radiation of chromosome aberrations in Tradescantia. *Journal of Genetics*, *44*(2–3), 216–245. https://doi.org/10.1007/bf02982830

Leeuwen, C. M., Oei, A. L., Crezee, J., Bel, A., Franken, N. A. P., Stalpers, L. J. A., & Kok, H. P. (2018). The alfa and beta of tumours: a review of parameters of the linear-quadratic model, derived from clinical radiotherapy studies. *Radiation Oncology*, *13*(1). https://doi.org/10.1186/s13014-018-1040-z

Michel, R., Françoise, I., Laure, P., Anouchka, M., Guillaume, P., & Sylvain, K. (2017). Dose to organ at risk and dose prescription in liver SBRT. *Reports of Practical Oncology &Amp; Radiotherapy*, *22*(2), 96–102. https://doi.org/10.1016/j.rpor.2017.03.001

Orton, C. G. (2001). High-dose-rate brachytherapy may be radiobiologically superior to low-dose rate due to slow repair of late-responding normal tissue cells. *International Journal of Radiation Oncology*Biology*Physics*, *49*(1), 183–189. https://doi.org/10.1016/s0360-3016(00)00810-5

Riaz, A., Awais, R., & Salem, R. (2014). Side Effects of Yttrium-90 Radioembolization. *Frontiers in Oncology*, *4*. https://doi.org/10.3389/fonc.2014.00198

Schuemann, J., McNamara, A. L., Ramos-Méndez, J., Perl, J., Held, K. D., Paganetti, H., Incerti, S., & Faddegon, B. (2018). TOPAS-nBio: An Extension to the TOPAS Simulation Toolkit for Cellular and Sub-cellular Radiobiology. *Radiation Research*, *191*(2), 125. https://doi.org/10.1667/rr15226.1

Sgouros, G., Bolch, W. E., Chiti, A., Dewaraja, Y. K., Emfietzoglou, D., Hobbs, R. F., Konijnenberg, M., Sjögreen-Gleisner, K., Strigari, L., Yen, T. C., & Howell, R. W. (2021). ICRU REPORT 96, Dosimetry-Guided Radiopharmaceutical Therapy. *Journal of the ICRU*, *21*(1), 1–212. https://doi.org/10.1177/14736691211060117

Son, S. H., Jang, H. S., Lee, H., Choi, B. O., Kang, Y. N., Jang, J. W., Yoon, S. K., & Kay, C. S. (2013). Determination of the α/β ratio for the normal liver on the basis of radiation-induced hepatic toxicities in patients with hepatocellular carcinoma. *Radiation Oncology*, *8*(1). https://doi.org/10.1186/1748-717x-8-61

Suntharalingam, N., Podgorsak, E. B., & Hendry, J. H. (2005). Basic Radiobiology. In *Review of Radiation Oncology Physics: A Handbook for Teachers and Students* (6th ed.). International Atomic Energy Agency.

Van de Wiele, C., Maes, A., Brugman, E., D'Asseler, Y., De Spiegeleer, B., Mees, G., & Stellamans, K. (2012). SIRT of liver metastases: physiological and pathophysiological considerations. *European Journal of Nuclear Medicine and Molecular Imaging*, *39*(10), 1646–1655. https://doi.org/10.1007/s00259-012-2189-6

Williams, M., Denekamp, J., & Fowler, J. (1985). A review of ratios for experimental tumors: Implications for clinical studies of altered fractionation. *International Journal of Radiation Oncology*Biology*Physics*, *11*(1), 87–96. https://doi.org/10.1016/0360-3016(85)90366-9

6. Acknowledgements

I would like to express my deepest gratitude for Dr. Alejandro Bertolet, who has been my advisor throughout my both my fellowship at MGH and my time writing this thesis. Without Dr. Bertolet and his previous work in radiobiology, this project could have never happened. Thank you for introducing me to medical physics and radiation oncology, a field I have come to love, and thank you for the many hours you have invested in helping me become a better physicist. I look forward greatly to our continued collaboration.

I would like to extend my sincere thanks to Prof. Janet Sheung, who also was integral in helping me pull this project together. Prof. Sheung has been my academic advisor since I first began studying physics, and I am grateful for her extensive guidance and kindness that have inspired me to pursue physics research.

Lastly, I would like to thank my family and friends who have unconditionally given me the support I've needed to pursue higher education and chase after my intellectual pursuits and passions. While it would be impossible to list everyone who has helped me get here, special thank you, in no particular order, to Mom, Pop-Pop, Nana, Dad, Xavier, Rukmini, Jon Joey, and Alexis. You all know how much I love you.